Reflectarray Nano-Dielectric Resonator Antenna Using Different Metals

Hend A. Malhat, Nermeen A. Eltresy, Saber H. Zainud-Deen, and Kamal H. Awadalla

Department of Electrical Engineering
Faculty of Electronic Eng., Menoufia University, 32952, Egypt
er_honida1@yahoo.com, anssaber@yahoo.com

Abstract ─ Nano-antennas have been introduced with wide bandwidth for faster data communications. The material properties of good conducting metals introduce plasmonic behavior at THz frequencies. The material property of good conducting metals using the Durde Lorentz model have been investigated. The radiation characteristics of nano-dielectric resonator antenna NDRA reflectarray at 633 nm have been investigated. A parametric study for the NDRA unit-cell dimensions and material has been introduced. Different types of metals are used as a supporting plane of the NDRA unit-cell. A NDRA with silver, copper, and aluminum supporting plane have been designed and analyzed for reflectarray antennas. A nano-reflectarray unit-cells with supporting plane having different metals have been introduced. Comparisons between the radiation characteristics of reflectarrays with different supporting plane metals have been illustrated. A compromise between the size, maximum gain, and operating bandwidth of the nano-reflectarray is investigated for terahertz applications. The finite integral technique is used to carry a full wave analysis to design a NDRA reflectarray.

Index Terms ─ DRA, nano-antenna, reflectarray.

I. INTRODUCTION

The radiation characteristics of a conventional radio-frequency RF antenna have been presented in detail [1]. Nano-antenna is a resonant device, which converts the EM wave into a localized energy at terahertz frequencies [2]. Recently, wide bandwidth nano-antennas have been introduced for faster information exchange. Nano-antennas have many applications including solar cells, on-chip wireless optical communication and biological imaging. Different forms of the microwave antennas such as dipole, monopole, Yagi-Uda, and bow-tie antenna have been investigated at the terahertz frequencies [3-6] which focus on resonant metallic nanostructures. The materials of nano-antennas are generally good conducting metals such as gold and silver [7]. The resonant structures of good conducting metals show electromagnetic resonances, when being excited by an incident light, this is called surface plasmon polariton resonances SPPRs. The optical properties of these metals are described by the Drude-Lorentz model, which considers both the free electrons contributions and harmonic oscillator SPPRs contributions [8]. However, only the high ohmic losses of metals at THz frequencies affect the radiation efficiency of nano-antennas [2]. The nano-antenna resonance length is not determined by the free space wavelength, but by the SPP wavelength in the metal [2]. The current distribution on the nano-antenna has a standing wave pattern similar to that of the RF antennas, but with non-uniform spacing between subsequent current lobes. Nano-antenna arrays introduce a superior directivity, field confinement, absorption cross-section and flexibility in beam shaping compared with single nano-antennas. Dielectric resonator antennas DRAs have many attractive features and applications at microwave frequencies [9]. The DRAs have different shapes such as a hemisphere, cylinder, or rectangular and are typically mounted on a metal layer regarded as perfect electric conductor. The DRAs are generally constructed from low-loss high-permittivity dielectric materials up to ε_r=100. To increase the efficiency of resonant nano-antennas, the low-loss high-permittivity dielectric materials available at THz frequencies are used. At THz frequencies, the wave penetrates the metals due to the plasmonic effect and the antenna scaling property is not valid. The radiation characteristics of the DRA at 633 nm have been investigated in [10]. High-gain microwave antennas have been employed in many applications such as radar and satellite communications. The parabolic reflector and phased array antenna have high gain, narrow main lobe and high power capacity, but suffer some disadvantages as high cost, large volume, and lossy feed networks. Reflectarray antenna combines the advantages of parabolic reflector and phased array and overcomes their disadvantages [11]. The reflectarray antenna consists of a primary source illuminating a planar surface composed of an array of unit-cells. The phase shift of each unit-cell is adjusted to collimate the reflected wave in the desired direction. Reflectarray suffers from feeder blocking effect, so it requires an offset feed to avoid blockage losses, which

Submitted On: March 10, 2015
Accepted On: June 1, 2015

leads to destroying the symmetry of the antenna aperture and increases the angle of incidence to some individual elements [12-14]. The detailed analysis of the radiation characteristics of NDRA element and NDRA reflectarray at 633 nm investigated in [10].

In this paper, the optical material properties of different conducting metals at THz frequencies have been investigated. A parametric study of the NDRA unit-cell for reflectarray at 633 nm has been introduced. The effect of changing the type of the metal material properties on the performance of the NDRA unit-cell is investigated. A 21×21 unit-cell elements NDRA reflectarray has been designed and analyzed using the finite integral technique based on the commercial software CST Microwave Studio [15,16]. Reflectarray with different metal supporting plane have been introduced. A comparison between the radiation characteristics of reflectarray with silver, copper and aluminum supporting plane has been presented.

II. MATERIAL PROPERTIES AT TERAHERTZ RANGE

At THz frequencies, the behavior of conventional metals properties behaves in a different way compared to the microwave frequencies [7]. In microwave frequency range the electric field inside the conductors is zero, which leads to perfect reflection from the surface of the metal, as the conductivity of metal is very high. However, at THz frequencies, the assumption of perfect conductor metals is not valid and the losses cannot be neglected [8]. The material properties in the THz range can be described by a free electron gas moving through a lattice of positive ions. The frequency dependent complex permittivity and the electrical conductivity of metal in the THz frequency range are described using Durde Lorentz model [8]:

$$\varepsilon_r = \varepsilon_1 + j\varepsilon_2 = [1 - \frac{\omega_p^2}{\omega\omega - j\vartheta_p}], \quad (1)$$

$$\sigma = \sigma_1 + j\sigma_2 = \varepsilon_o \frac{\omega_p^2}{j\omega + \vartheta_p}, \quad (2)$$

where ε_1 is the real part of permittivity and is a measure of how much energy from an external field is stored in a material. ε_2 is the imaginary part of permittivity loss factor. It is a measure of how dissipative or lossy a material is to an external field, ε_o is the dielectric constant of vacuum, ω is the angular frequency of the electromagnetic wave, ϑ_p is the angular collision frequency, and ω_p is the electron plasma angular frequency [8]:

$$\omega_p = \sqrt{n_e q^2/\varepsilon_o m_e} = 56.40\sqrt{n_e}, \quad (3)$$

where n_e is the free electron density, m_e is the electron mass, and q is the charge of the electron. Figure 1 shows the variation of electric permittivity ε, and the conductivity σ, versus frequency in the THz range of gold, copper, silver and aluminum. The electrical permittivity and conductivity of all metals take an exponential variation with frequency. ε_1 *and* σ_2 are increased by increasing frequency negative with reduced magnitude with higher frequency while ε_2 and σ_1 are decreased in magnitude by increasing frequency. The skin depth is representing how deep the electromagnetic wave can penetrate the material surface [8]:

$$\delta(\omega) = \frac{2c\sqrt{\frac{\varepsilon_1}{2} + \frac{1}{2}\sqrt{\varepsilon_1^2 + \varepsilon_2^2}}}{\omega\varepsilon_2}, \quad (4)$$

where c is the speed of light. The variations of skin-depth versus frequency for different types of metals are shown in Fig. 2. At 474 THz, the skin depth is 32 nm for gold, 28 nm for copper, 24.5 nm for silver and 17 nm for aluminum.

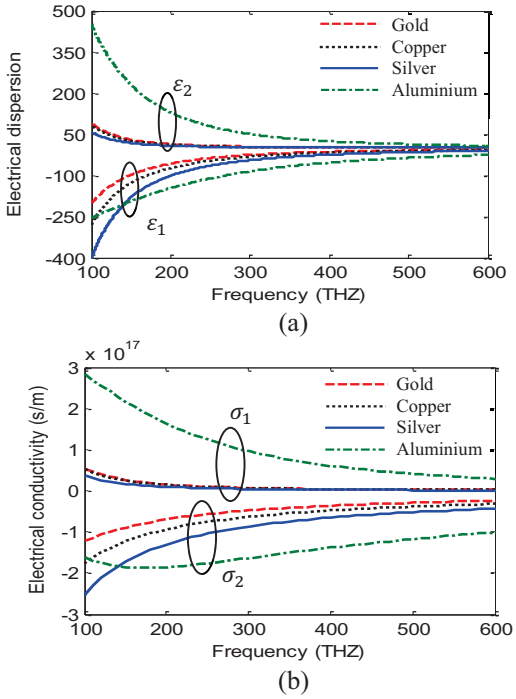

Fig. 1. The variations of complex permittivity and electrical conductivity versus frequency for different types of metals: (a) electrical dispersion, and (b) electrical conductivity.

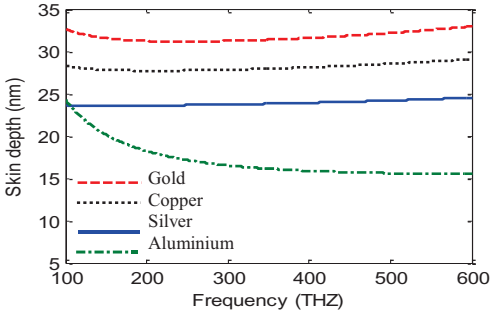

Fig. 2. The skin depth variation versus frequency.

III. THEORY OF REFLECTARRAY ANTENNA

The reflectarray operation can be seen as a phased array with spatial feed located at (x_f, y_f, z_f) from the array aperture. For the reflectarray located in x-y plane, the wave is reflected from each unit-cell at direction $(\theta_0,\emptyset_o)$ suffer from additional phase shift due to the position of the element in the array (x_{ci}, y_{ci}) and spacing between the cell element and the feeding horn d_{ij}, as shown in Fig. 3. To collimate the reflected wave at direction $(\theta_0,\emptyset_o)$ each unit-cell require a compensation phase:

$$\varphi_{ij}(x_{ci}, y_{ci}) = k_o d_{ij} + \emptyset_{cij}, \quad (5)$$

where $k_o = 2\pi/\lambda_o$ is the wave number, d_{ij} is given by [12]:

$$d_{ij} = \sqrt{x_{ci} - x_f{}^2 + \left(y_{ci} - y_f\right)^2 + z_f{}^2}, \quad (6)$$

and $\emptyset_{cij}$ is the phase shift due to the location of the unit-cell in the array:

$$\varphi_{cij} = -x_{ci} sin\theta_0 cos\emptyset_o - y_{ci}\, sin\theta_0\, sin\emptyset_o. \quad (7)$$

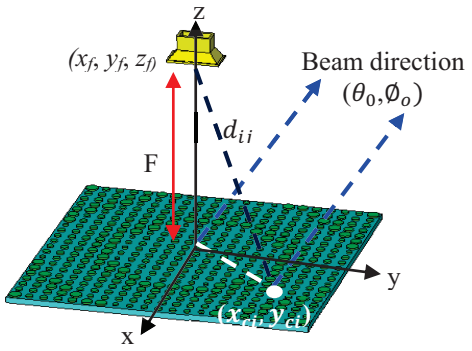

Fig. 3. The detailed structure of the reflectarray configuration.

IV. DESIGN OF NDRA REFLECTARRAY WITH SILVER SUPPORTING PLANE

The unit-cell of nano dielectric resonator reflectarray consists of a NDRA made of titanium dioxide TiO_2, with anisotropic frequency independent dielectric permittivity of 8.29 in x- and y-axis directions and 6.71 in z-axis direction. The estimated loss tangent is 0.001 [10]. The NDRA has a cylindrical shape with radius R and height h_d placed on a square ground plane with side length L and thickness h as shown in Fig. 4 (a). To calculate the required reflection coefficient phase compensation in each unit-cell, the unit-cell is put in a waveguide simulator [13]. The perfect electric and magnetic wall boundary conditions are posted onto the sides of the surrounding waveguide, and result in an infinite array. A linearly polarized plane wave was applied as the far-field excitation of the unit-cells inside the waveguide simulator and only normal incidence angle is considered. There are several limitations to the infinite array approach. First, all elements of the reflectarray/transmitarray are identical; this is not the case in the real reflectarray/transmitarray in which the diameters of the NDR in each cell element must vary according to the required phase compensation. Secondly, the reflectarray/transmitarray itself is not infinite in extent. Finally, only normal incidence is considered. However, the plane wave has an oblique angle on the real array element, but the phase variation is nearly the same for incidence angles up to 30° [14]. Different types of metals are used for ground plane as silver, gold, copper, and aluminium. The properties of the ground plane metals are determined using Eq. (1) at 474 THz and are listed in Table 1. The required compensation phase of the reflection coefficient for each unit-cell is achieved by varying the NDRA radius R. Figure 5 shows the variation of the reflection coefficient magnitude and phase versus the NDRA radius at 474 THz for different types of ground plane metals. The gold ground plane has the worst reflection coefficient variation from -30.4 to -2.9, while the silver ground plane gives the best reflection coefficient magnitude varies from -5.8 to -1.7 dB for the NDRA radius varying from 85 nm to 170 nm. This is because the conductivity of the aluminum material is higher than that of the silver material at 474 THz as appeared in Fig. 1 (b), and the penetration depth in aluminum ground plate is higher than that of silver as shown in Fig. 2. The phase of the reflection coefficient span of variation is 360° for the silver, 19° for gold, 215° for the copper, and 136° for the aluminum ground plate. The silver material has the best performance for the reflectarray unit-cell with reflection coefficient magnitude variation from -5.8 to -1.7 dB, and phase variation from 0 to 360 degrees.

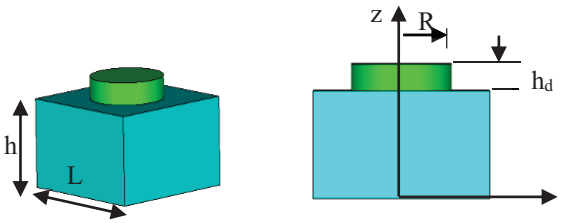

Fig. 4. The detailed structure of the NDRA reflectarray unit-cell: (a) 3-D view, and (b) side view.

Table 1: The optical properties of the different types of metals at 474 THz [17]

Metal	ω_p (rad/sec)	υ_p (rad/sec)	δ (nm)
Silver	1.28×10^{16}	9.19×10^{13}	24.5
Gold	0.98×10^{16}	2.8×10^{14}	32
Copper	1.13×10^{16}	3.2×10^{14}	28
Aluminum	2.3×10^{16}	1.04×10^{15}	17

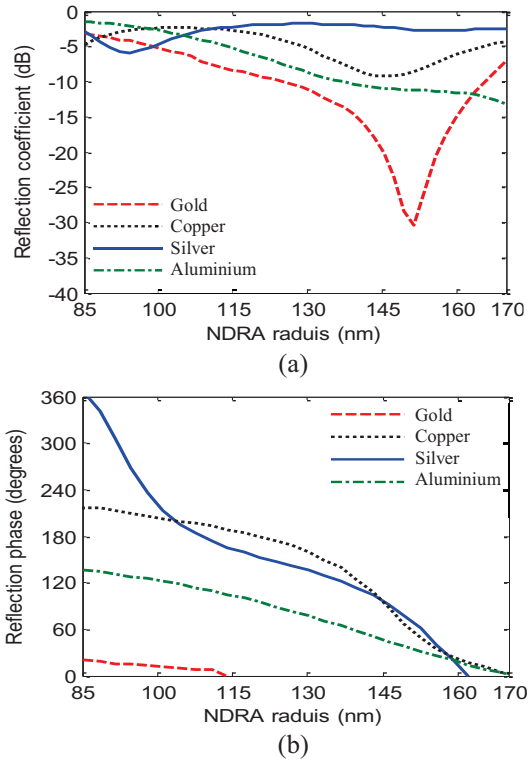

Fig. 5. The variation of the reflection coefficient magnitude and phase versus the NDRA radius at 474 THz: (a) reflection coefficient magnitude, and (b) reflection coefficient phase magnitude.

Figure 6 shows the effect of changing the silver ground plane thickness of the unit-cell on the variation of the reflection coefficient magnitude and phase. By increasing the ground plane thickness, the reflection coefficient magnitude is decreased and the reflection coefficient phase variation is increased to achieve 360 degrees. A compromise between the magnitude and phase of the reflection coefficient has been made. A ground plane thickness of 200 nm has been chosen for reflection coefficient magnitude variation from -1.7 to -5.8 and 360 degrees phase variations. The electric field distribution on the unit-cell of the NDRA reflectarray with silver supporting plane h=200 nm, h_d =50 nm, and R=130 nm is shown in Fig. 7. The incident plane wave penetrate the silver supporting plane at a distance equal to the skin depth at this frequency 24.5 nm and reflects back to the source direction. The reflection occurs because the thickness of the silver supporting plane is much bigger than the silver skin depth about 8.16 δ.

A 21×21 unit-cell elements NDRA reflectarray is constructed using silver plane with L=350 nm, h=200 nm, and h_d =50 nm as shown in Fig. 8. The array has total dimensions of 7.35×7.35 μm^2. A linearly polarized pyramidal nano-horn antenna is used to feed the NDRA reflectarray located at 8.133 μm from the array aperture. The nano-horn antenna is constructed from gold with L_h=487.5 nm, and aperture size a×b of 810 nm × 1275 nm. The nano-horn antenna has a maximum gain of 11.1 dBi at 474 THz. The E- and H-plane radiation patterns at 474 THz of the nano-horn and the NDRA reflectarray with different plane thickness h=30, 70 and 200 nm are shown in Fig. 9. The maximum gain of the NDRA reflectarray is increased by increasing the plane thickness and the SLL is decreased. For h=200 nm, the first SLLs are -17.9 dB and -15.1 dB in E- and H-plane respectively. The HPBW of the NDRA reflectarray is 4.5 degrees in E-plane and 4.7 degrees in H-plane compared to 40.3 degrees in E-plane and 41.3 degrees in H-plane for the nano-horn antenna.

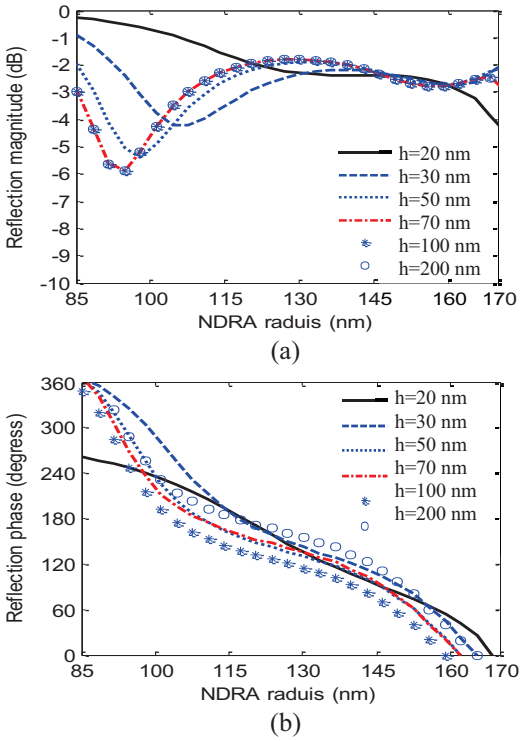

Fig. 6. The variations of the reflection coefficient magnitude and phase versus the NDRA radius: (a) reflection coefficient magnitude, and (b) reflection coefficient phase magnitude.

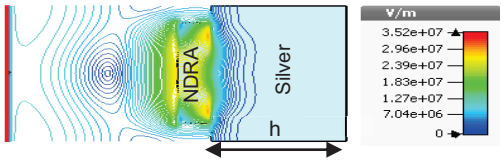

Fig. 7. The electric field distribution on the unit-cell with silver supporting plane, h=200 nm, L=350 nm, h_d =50 nm and R=130 nm.

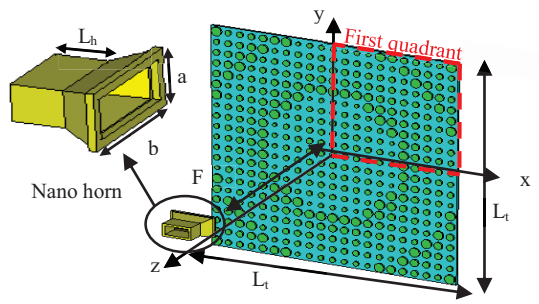

Fig. 8. The 21×21 unit-cell elements NDRA reflectarray with silver supporting plane.

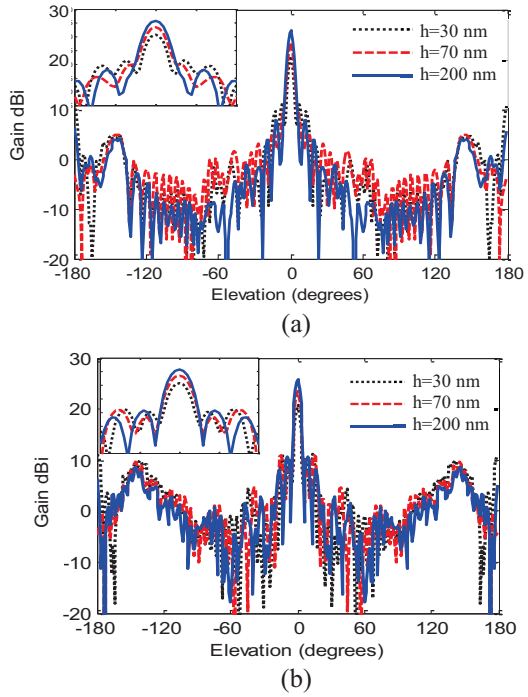

Fig. 9. The gain patterns plot for a 21×21 NDRA reflectarray with silver supporting plane for variable ground plane thickness.

V. DESIGN OF NDRA REFLECTARRAY WITH COPPER SUPPORTING PLANE

The NDRA unit-cell with copper supporting plane has the same construction as shown in Fig. 4. The supporting plane is replaced by copper material. The dimensions of the NDRA unit-cell with copper supporting plane is designed and optimized to operate at 474 THz. The unit-cell dimensions are h_d =105 nm placed on a square copper ground plane with side length L=350 nm, thickness h=200 nm and variable values for NDRA radius R. The incident wave penetrate the copper supporting plane down to the skin depth and reflects back to the source. The variations of the reflection coefficient magnitude and phase for the unit-cell with copper supporting plane are shown in Fig. 10. A 300° phase shift of the reflection coefficient unit-cell is achieved by varying the NDRA radius R from 75 to 175 nm. While the reflection coefficient magnitude is changed from -1.8 to -5.6 dB at 474 THz. A 21×21 unit-cell elements NDRA reflectarray with copper supporting plane of thickness h=200 nm, length of 7.35 μm and NDRA height of 105 nm is constructed. The NDRA reflectarray has maximum gain of 27.2 dBi with front to back ratio of 21 dB. The gain variation versus frequency for the NDRA reflectarray with copper supporting plane and the nano-horn are shown in Fig. 11. The 1-dB gain bandwidth is 35 dB.

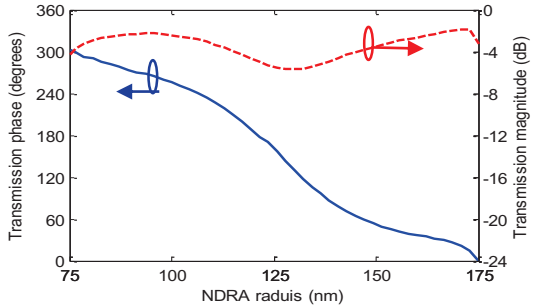

Fig. 10. The variation of the reflection coefficient phase and magnitude versus the NDRA radius at 474 THz.

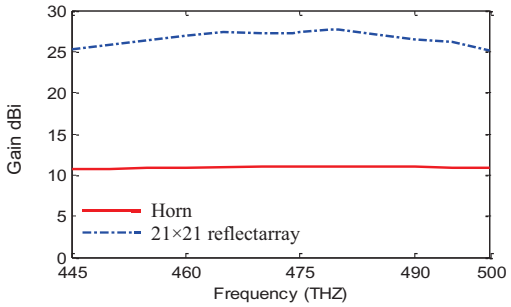

Fig. 11. The gain variation versus frequency for a 21×21 NDRA reflectarray with copper supporting plane at L=350 nm, h=200 nm, and h_d=105 nm.

VI. DESIGN OF NDRA REFLECTARRAY WITH ALUMINUM SUPPORTING PLANE

A NDRA reflectarray unit-cell with aluminum supporting plane with side length L=350 nm, thickness h=200 nm, and hd=170 nm operated at 474 THz is investigated. Figure 12 (a) shows the electric field distribution on NDRA reflectarray unit-cell with aluminum supporting plane at 474 THz with h=200 nm, hd=170 nm and R=130 nm. The reflection coefficient magnitude and phase variations versus the NDRA radius are shown in Fig. 12 (b). A 360° phase variation and reflection coefficient magnitude variation from -4.7 to -5.4 dB are achieved. The gain variation versus

frequency for the NDRA reflectarray with aluminum supporting plane is shown in Fig. 13.

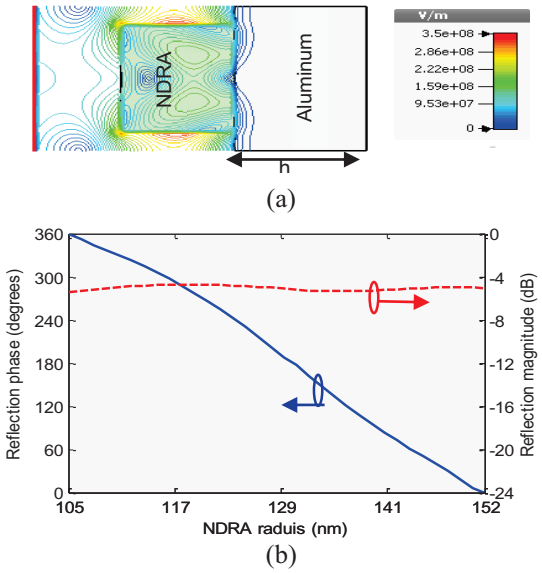

Fig. 12. (a) The electric field distribution on the NDRA reflectarray unit-cell with aluminum supporting plane, and (b) the reflection coefficient phase and magnitude versus the NDRA radius at 474 THz.

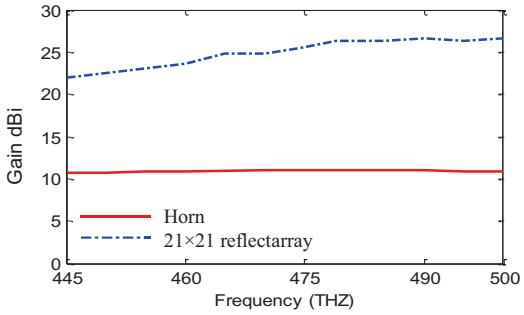

Fig. 13. The gain variation versus frequency for a 21×21 NDRA reflectarray with aluminum supporting plane.

VII. COMPARISON BETWEEN NDRA REFLECTARRAYS WITH DIFFERENT METAL SUPPORTING PLANES

The E-and H-plane gain patterns for 21×21 NDRA reflectarrays with silver, copper, and aluminum supporting planes are shown in Fig. 14. The reflectarray with copper supporting plane has the maximum gain of 27.8 dBi with lower HPBW of 4.4° due to the higher reflection coefficient magnitude relative to the other metals. The reflectarray with aluminum supporting plane has the lower gain and the higher bandwidth, due to the increase in the NDRA height with variation of its relative permittivity in the z-direction. Table 2 lists a comparison between the radiation characteristics of the reflectarrays with different metals supporting plane. A compromise between gain, 1-dB bandwidth, SLL, and HPBW has been applied for choosing the appropriate reflectarray for THz applications.

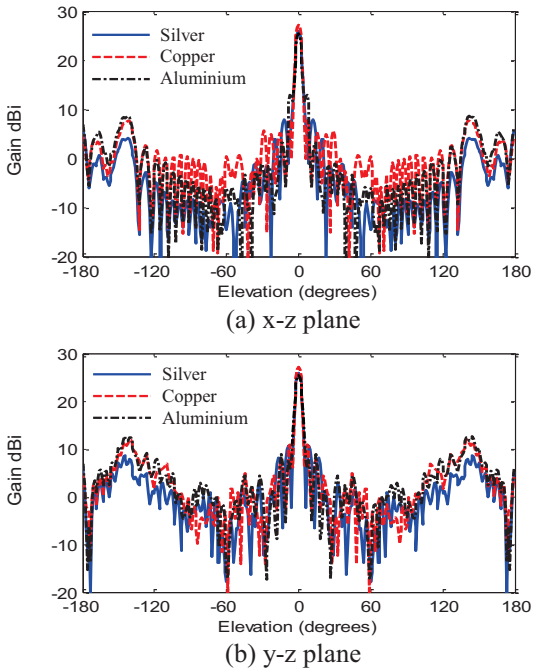

Fig. 14. The gain radiation patterns plot for a 21×21 NDRA reflectarray with different supporting plane nano metals.

Table 2: Comparison between the radiation characteristics of NDRA reflectarrays with different metals supporting planes

Material	Silver	Copper	Aluminum
Gain dBi	25.8	27.2	25.4
1-dB BW	30 THz	35 THz	40 THz
SLL (dB)	-17.9	-19.4	-12.51
HPBW (degrees)	4.5	4.5	4.3

VIII. CONCLUSION

The use of NDRA in the design of nano-reflectarray for terahertz application at 633 nm is introduced. The reflectarray unit-cell consists of a cylindrical NDR on a square ground plane of a good conductor. A parametric study for the unit-cell dimensions has been introduced. The gold ground plane has got the worst reflection coefficient, while the silver ground plane gives the best reflection coefficient magnitude. A compromise between the magnitude and phase of the reflection coefficient has been made. A silver ground plane thickness of 200 nm has been chosen for reflection coefficient magnitude variation from -1.7 to -5.8 dB and 360 degrees phase variation. A 21×21 unit-cell elements NDRA reflectarray is constructed using silver supporting plane

with L=350 nm, h=200 nm, and hd=50 nm. The maximum gain of the NDRA reflectarray is increased by increasing the plane thickness and the SLL is decreased.

REFERENCES

[1] A. C. Balanis, *Antenna Theory Analysis and Design*, 3rd edition, John Wiley & Sons, USA, 2012.

[2] M. Agio, "Optical antennas as nanoscale resonators," *Nanoscale Journal*, vol. 3, pp. 692-706, 2011.

[3] P. Muhlschlegel, H. J. Eisler, O. J. F. Martin, B. Hecht, and D. W. Pohl, "Resonant optical antennas," *Science Magazine*, vol. 308, pp. 1607-1609, Jun. 2005.

[4] T. H. Taminiau, F. B. Segerink, R. J. Moerland, L. Kuipers, and N. F. Hulst, "Near-field driving of a optical monopole antenna," *Journal of Optics A: Pure and Applied Optics*, vol. 9, pp. 315-321, Aug. 2007.

[5] I. S. Maksymov, A. E. Miroshnichenko, Y. S. Kivshar, "Actively tunable optical Yagi-Uda nanoantenna with bistable emission characteristics," *Optics Express*, vol. 8, pp. 8929-8938, Feb. 2012.

[6] H. Fischer and O. J. Martin, "Engineering the optical response of plasmonic nanoantennas," *Optics Express*, vol. 16, no. 12, pp. 9144-9154, Jun. 2008.

[7] R. Vajtai, *Hand Book of Nanomaterials*, Springer Handbooks, New York, USA, 2013.

[8] N. Kumar, "Spontaneous emission rate enhancement using optical antennas," *Ph.D. Thesis*, University of California, Berkeley, USA, 2013.

[9] K. M. Luk, K. W. Leung, and J. R. James, *Dielectric Resonator Antennas*, Research Studies Press, Hertfordshire, England, 2002.

[10] L. Zou, "Dielectric resonator antennas from multifunction microwave devices to optical nano-antennas," *Ph.D. Thesis*, School of Electrical and Electronic Engineering, University of Adelaid, Australia, Mar. 2013.

[11] S. H. Zainud-Deen, H. A. Malhat, S. M. Gaber, M. Ibrahim, and K. H. Awadalla, "Plasma reflectarray," *Plasmonics*, vol. 8, no. 3, pp. 1469-1475, Sept. 2013.

[12] J. Huang and J. A. Encinar, *Reflectarray Antennas*, John Wiley and Sons, Inc., New Jersy, USA, 2007.

[13] S. H. Zainud-Deen, H. A. Malhat, S. M. Gaber, and K. H. Awadalla, "Perforated nanoantenna reflectarray," *Progress in Electromagnetics Research M, PIER M*, vol. 29, pp. 253-265, 2013.

[14] H. A. Malhat, S. H. Zainud-Deen, and S. M. Gaber, "Circularly polarized graphene based transmitarray for terahertz applications," *Progress in Electromagnetics Research M, PIER M*, vol. 36, pp. 185-191, 2014.

[15] R. Schumann, T. Weiland, W. H. Schilders, E. J. Maten, and S. H. Houben, "Recent advances in finite integration technique for high frequency applications," *Scientific Computing in Electrical Engineering*, vol. 4, pp. 46-57, 2004.

[16] CST Microwave Studio, http://www.cst.com/.

[17] M. A. Ordal, L. L. Long, R. J. Bell, S. E. Bell, R. R. Bell, R. W. Alexander, Jr., and C. A. Ward, "Optical properties of the metals Al, Co, Cu, Au, Fe, Pb, Ni, Pd, Pt, Ag, Ti, and W in the infrared and far infrared," *Applied Optics*, vol. 22, no. 7, pp. 1099-11201, Apr. 1983.

Hend Abd El-Azem Malhat was born in Menouf, Egypt, on December 12, 1982. She received the B.Sc. and M.Sc. degrees from Menoufia University in 2004 and 2007, respectively. She received her Ph.D. degree in Antenna Engineering from Menoufia University, Egypt in 2011. She is currently an Associat Professor in the Department of Electrical and Electronic Engineering in the Faculty of Electronic Engineering, Menoufia University, Egypt. Her research interest at present include graphene antennas, plasma antennas, wavelets technique, transmitarray, reflectarray and RFID.

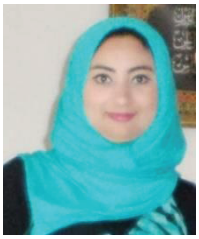

Nermeen A. Elteresy was born in Menouf, Egypt, on Sebtemer 29, 1990. She received the B.Sc. degree from Menoufia University in 2012. She is currently working toward her M.Sc. degree in Antenna Engineering from Menoufia University. Her research interest at present include nano-antennas, DRA, transmitarray, and reflectarray.

Saber Helmy Zauind-Deen was born in Menouf, Egypt, on November 15, 1955. He received the B.Sc. and M.Sc. degrees from Menoufia University in 1973 and 1982, respectively, and the Ph.D. degree in Antenna Engineering from Menoufia University, Egypt in 1988. He is currently a Professor in the Department of Electrical and Electronic Engineering in the Faculty of Electronic Engineering, Menoufia University, Egypt. His research interest at present include microstrip and leaky wave antennas, DRA, RFID, optimization techniques, FDFD and FDTD, scattering problems and breast cancer detection.

Kamal H. Awadalla was born in El-Santa - Gharbiya - Egypt, on February 1, 1943. He received the B.Sc. and M.Sc. from the Faculty of Engineering, Cairo University, Egypt, in 1694 and 1972, respectively, and the Ph.D. degree from the University of Birmingham, UK. in 1978. He is currently a Professor Emeritus in the Dept. of Electrical and Electronic Engineering in the Faculty of Electronic Engineering, Menoufia University, Egypt. His research interest at present include microstrip and leaky wave antennas, DRA, RFID, optimization techniques.